HOW DOES NONLOCAL DISPERSAL AFFECT THE SELECTION AND STABILITY OF PERIODIC TRAVELING WAVES?*

JONATHAN A. SHERRATT†

Abstract. In ecology a number of spatiotemporal datasets on cyclic populations reveal periodic traveling waves of abundance. This calls for studies of periodic traveling wave solutions of ecologically realistic mathematical models. For many species, such models must include long-range dispersal. However, mathematical theory on periodic traveling waves is almost entirely restricted to reaction-diffusion equations, which assume purely local dispersal. I study integrodifferential equation models in which dispersal is represented via a convolution. The dispersal kernel is assumed to be of either Gaussian or Laplace form; in either case it contains a parameter scaling the width of the kernel. I show that as this parameter tends to zero, the integrodifferential equation asymptotically approaches a reaction-diffusion model. I exploit this limit to determine the effect of a small degree of nonlocality in dispersal on periodic traveling wave properties and on the selection of a periodic traveling wave solution by localized perturbation of an unstable steady state. My analysis concerns equations of "λ–ω" type, which are the normal form of a large class of oscillatory systems close to a Hopf bifurcation point. I finish the paper by showing how my results can be used to determine the effect of nonlocal dispersal on spatiotemporal dynamics in a predator-prey system.

Key words. wavetrain, integrodifferential equation, dispersal kernel, invasion, periodic traveling wave, oscillatory systems, cyclic population, absolute stability

AMS subject classifications. 35R09, 35C07, 92D40

DOI. 10.1137/17M1142168

1. Introduction. Many natural populations undergo regular cycles of abundance. Investigation of the population dynamics of such cyclic populations is an active research area because of well-documented evidence that in many cases their demographic parameters are shifting in response to climate change [1, 2]. A particular focus of recent research has been the spatial distribution of cyclic populations, with field studies documenting periodic traveling waves (PTWs) in a number of natural populations including voles [3, 4], moths [5], and red grouse [6] (see [7] for additional examples). Spatially extended oscillatory systems have a family of PTW solutions [8], and the initial and boundary conditions select one member of the family [11, 12, 13, 14]. Solution of this wave selection problem is crucial for a thorough understanding of the PTWs seen in the field. In this paper I focus on PTW selection by localized perturbations of an unstable steady state.

There is an extensive mathematical literature on PTW generation [15, 18, 17, 12, 16, 19, 13, 14], but it concerns almost exclusively reaction-diffusion equations. Although such equations are widely used in ecological modeling (see, for example, [20]), their realism is limited by the use of diffusion to represent dispersal. Rare long-distance dispersal events play a key role in the spread of many natural populations, and thus it is more appropriate to use a nonlocal term: spatial convolution with a dispersal kernel. Estimation of dispersal kernels is at its most refined in plants; for example, the recent review of Bullock et al. [21] lists the most appropriate kernels for 144 plant species. However, long-range dispersal is also important for animals. For

---

†Department of Mathematics and Maxwell Institute for Mathematical Sciences, Heriot-Watt University, Edinburgh EH14 4AS, UK (j.a.sherratt@hw.ac.uk).

example, Fric and Konvicka [22] studied dispersal kernels for three species of butterfly, and Byrne et al. [23] discussed the potential importance of long-range dispersal of European badgers for the spread of bovine tuberculosis.

Many of the theoretical models used in applied ecology involve nonlocal dispersal, and the aim of this paper is to bridge the gap between such models and the mathematical work on PTW generation in reaction-diffusion systems. The results presented here build directly on two previous papers of mine [24, 25]. In [24] I studied PTWs in integrodifferential equations with "λ–ω" kinetics (details below), which arise as the normal form of an oscillatory system close to a standard supercritical Hopf bifurcation, and which offer considerable mathematical simplicity compared to general kinetics. In [24] I derived the form of PTW solutions of these equations, and conditions for their stability, when the dispersal kernel is of either Gaussian or Laplace form (defined below). In [25] I focused on PTW generation, with the central result being a theorem on PTW selection, and I also made a brief numerical comparison between PTW selection in a predator-prey model with nonlocal dispersal and the corresponding reaction-diffusion model. In the present paper I undertake a much more detailed version of this comparison. I begin by showing that for a dispersal kernel of Gaussian form, the integrodifferential equation reduces to a reaction-diffusion system to leading order in a suitable asympotic limit; the case of a Laplace kernel is discussed later in the paper. Focusing again on the case of λ–ω kinetics, I exploit this to derive leading order corrections to the PTW that is selected by localized perturbation of an unstable steady state, and its stability. I also consider the absolute stability of the selected PTW, which is a key determinant of the resulting spatiotemporal dynamics. Finally I apply my results to a model for predator-prey interaction.

2. Relating local and nonlocal dispersal. The study of PTW solutions of models with nonlocal dispersal is very much in its infancy, and the general case is currently out of reach. Throughout this paper I restrict attention to models satisfying two simplifying assumptions: (i) the dispersal is scalar, meaning that the dispersal kernel and the coefficient are the same for each interacting population; (ii) the kinetic parameters are close to a Hopf bifurcation of standard supercritical type. These assumptions are made for mathematical simplicity. From the viewpoint of ecological applications, scalar dispersal is appropriate in some situations, for example, for interacting microscopic aquatic populations [26]; however, in terrestrial or macroscopic marine predator-prey systems the predators typically disperse more rapidly than their prey [27, 28]. Being close to a Hopf bifurcation point implies that oscillations are of low amplitude, which is certainly relevant to applications, although many population cycles involve large variations in abundance. Nevertheless, a study making assumptions (i) and (ii) is valuable as a first stage in understanding PTWs in integrodifferential equation models.

For scalar dispersal, the normal form of an oscillatory system with nonlocal dispersal close to a standard supercritical Hopf bifurcation in the kinetics has the form

$$\partial u/\partial t = \delta \left[\int_{y=-\infty}^{y=\infty} K(x-y)u(y,t)dy - u \right] + (\lambda_0 - \lambda_1 r^2)u - (\omega_0 + \omega_1 r^2)v \,,$$

(2.1)

$$\partial v/\partial t = \delta \left[\int_{y=-\infty}^{y=\infty} K(x-y)v(y,t)dy - v \right] + (\omega_0 + \omega_1 r^2)u + (\lambda_0 - \lambda_1 r^2)v$$

[29, 30, 31, 32], and it is this system of equations that will be the focus of my study. Here $r = \sqrt{u^2 + v^2}$ and δ, λ_0, λ_1, ω_0, and ω_1 are constants with $\delta, \lambda_0, \lambda_1 > 0$.

In the context of an ecological application, these constants would be functions of the ecological parameters and u and v would be functions of the population densities; these functional dependencies can be derived using standard normal form theory [33, 31, 32] (see also section 6).

The inclusion of the dispersal parameter δ is actually unnecessary because it can be removed by suitable rescalings of t, λ_0, λ_1, ω_0, and ω_1. However, I include it because it simplifies the comparison between (2.1) and the corresponding model with local dispersal. The dispersal kernel $K(y)$ must be ≥ 0 for all y and must satisfy $\int_{-\infty}^{\infty} K(y)\, dy = 1$ so that the dispersal term conserves population. I will focus on two specific forms,

$$(2.2) \qquad \text{Gaussian kernel:} \quad K(s) = \left(1/\epsilon\sqrt{\pi}\right)\exp\left(-s^2/\epsilon^2\right),$$

$$(2.3) \qquad \text{Laplace kernel:} \quad K(s) = (1/2\epsilon_l)\exp\left(-|s|/\epsilon_l\right)$$

(ϵ, $\epsilon_l > 0$), which are probably the most widely used kernels in ecological and epidemiological applications (e.g., [34, 35, 36]). I will consider the Gaussian kernel (2.2) in the bulk of the paper, with corresponding results for the Laplace kernel discussed in section 7.

The central objective of my study is to compare PTW generation by localized disturbance of the (unstable) steady state $u = v = 0$ in (2.1) and in the corresponding model with local dispersal:

$$
\begin{aligned}
\partial u/\partial t &= \partial^2 u/\partial x^2 + (\lambda_0 - \lambda_1 r^2)u - (\omega_0 + \omega_1 r^2)v\,, \\
(2.4) \\
\partial v/\partial t &= \partial^2 v/\partial x^2 + (\omega_0 + \omega_1 r^2)u + (\lambda_0 - \lambda_1 r^2)v\,.
\end{aligned}
$$

This generic oscillatory reaction-diffusion system was first studied in the 1970s [8], and the existence and stability of its PTW solutions are known in detail [8, 11, 17]. I will begin by showing that (2.1) with (2.2) reduces to (2.4) as the parameter $\epsilon \to 0$, provided that the dispersal coefficient δ is chosen appropriately; a similar argument was used in [37].

For the Gaussian kernel (2.2), the dispersal term (for u, say) is

$$
\delta\left[\frac{1}{\epsilon\sqrt{\pi}}\int_{s=-\infty}^{s=\infty} e^{-s^2/\epsilon^2} u(s+x,t)ds - u(x,t)\right]
$$

$$
= \delta\left[\frac{1}{\epsilon\sqrt{\pi}}\int_{s=-\infty}^{s=\infty} e^{-s^2/\epsilon^2}\left\{u(x,t) + su_x(x,t) + \frac{1}{2}s^2 u_{xx}(x,t) + \cdots\right\}ds - u(x,t)\right]
$$

$$
\sim \frac{\delta u_{xx}(x,t)}{2\epsilon\sqrt{\pi}}\int_{s=-\infty}^{s=\infty} s^2 e^{-s^2/\epsilon^2}ds = \frac{1}{4}\epsilon^2\delta u_{xx}(x,t)
$$

using Watson's lemma. Here the subscript x denotes a partial derivative. Therefore taking $\delta = 4/\epsilon^2$ means that the (nonlocal) dispersal term in (2.1) approaches the (local) diffusive dispersal term in (2.4) asymptotically as $\epsilon \to 0$. It is this direct correspondence between the models with local and nonlocal dispersal that enables a detailed comparison of PTW behavior.

3. Previous results on periodic traveling waves for nonlocal dispersal. The starting point for my work is the results in [24, 25] on PTWs in (2.1) with (2.2) or (2.3), which I now summarize.

- PTW solutions of (2.1) with (2.2) or (2.3) have the form $u = R\cos\left[(\omega_0 + \omega_1 R^2)t \pm \alpha x\right]$, $v = R\sin\left[(\omega_0 + \omega_1 R^2)t \pm \alpha x\right]$, where the amplitude $R\ (> 0)$ and the wavenumber α (of either sign) are related by

$$(3.1) \qquad \lambda_0 - \lambda_1 R^2 = \delta\left[1 - \int_{s=-\infty}^{s=\infty} K(s)\cos\alpha s\, ds\right]$$

  (equation (2.2) of [24]). When $\lambda_0 \geq \delta$ this implies that a PTW exists for all α, while for $\lambda_0 < \delta$ PTWs exist for α below a critical value at which $R = 0$.
- The PTW is stable as a solution of (2.1) if and only if

$$(3.2)$$
$$\delta\left[1 + \left(\frac{\omega_1}{\lambda_1}\right)^2\right] \cdot \left[\int_{s=-\infty}^{s=\infty} sK(s)\sin\alpha s\, ds\right]^2 < \lambda_1 R^2 \int_{s=-\infty}^{s=\infty} s^2 K(s)\cos\alpha s\, ds$$

  (Theorems 2.1, 3.2, and 3.3 of [24]). For both kernels, this implies a critical value of $|\alpha|$ above/below which waves are unstable/stable.
- Numerical simulations show that a localized disturbance of the steady state $u = v = 0$ generates transition fronts moving in the positive and negative x directions with constant speed. Behind the fronts PTWs develop, which have the same amplitude but opposite direction behind the fronts moving in the positive and negative x directions.
- The PTW selected behind the transition front moving in the positive x direction satisfies

$$(3.3) \qquad\qquad\qquad c\alpha = -\omega_1 R^2\,,$$

  where c is the front (or spreading) speed (Theorem 3.1 of [25]). The combination of this equation and (3.1) has a unique solution for α whose sign is opposite to that of ω_1. Intuitive arguments based on theorems on front propagation in simpler integrodifferential equation systems [35, 38] suggest that the spreading speed c satisfies

$$(3.4) \qquad\qquad c = \min_{\eta>0} \frac{1}{\eta}\left[\delta\int_{s=-\infty}^{s=\infty} K(s)e^{\eta s}\, ds - \delta + \lambda_0\right]$$

  (equation (3.4) of [25]); however, a formal proof of this is lacking. Note that $M(\eta) \equiv \int_{s=-\infty}^{s=\infty} K(s)e^{\eta s}\, ds$ is known as the moment generating function of the kernel $K(.)$.

Figure 3.1 illustrates the generation of PTWs by localized perturbation of $u = v = 0$ in (2.1). In (a) and (b) the values of ω_1 have opposite signs, and consequently the PTWs move in opposite directions. In (c) and (d) the selected PTW is unstable; in (c) PTWs are generated but they then destabilize, with the long-term behavior being spatiotemporal disorder. In (d) spatiotemporal disorder occurs without any preceding PTWs; nevertheless PTW selection is the key process underlying this behavior, as I will show.

From the viewpoint of applications to predator-prey systems, the solutions illustrated in Figure 3.1 correspond to the spreading of PTWs into predators and prey at the coexistence steady state. In applications this is relevant when a change in environmental conditions alters the stability of the coexistence state. The local dynamics then change from noncyclic to cyclic; an example of this is given in the work
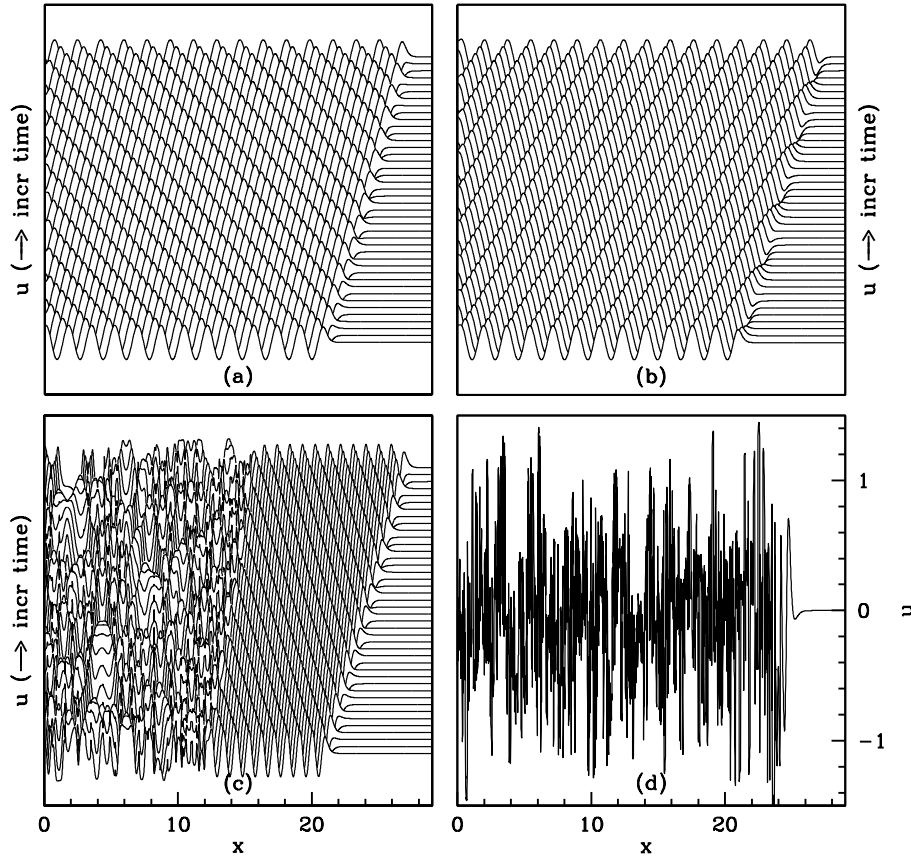
Fig. 3.1. *Examples of PTW generation by a localized disturbance of the steady state $u = v = 0$ in the λ–ω system (2.1). In (a) and (b) the selected PTW is stable, moving in the opposite direction to the spread of the PTWs in (a) and the same direction in (b). In (c) the PTW is unstable; a band of PTWs is visible, followed by spatiotemporal disorder. In (d) spatiotemporal disorder develops immediately: in this case a PTW is selected but it is absolutely unstable in the frame of reference moving with the spreading speed (see section 5). The equations were solved numerically by discretizing in space using a uniform grid ($\delta x = 0.012$) and calculating the spatial convolutions using fast Fourier transforms. This gives a system of ordinary differential equations that was solved using the stiff ODE solver ROWMAP [39] (http://numerik.mathematik.uni-halle.de/forschung/ software/), with relative and absolute error tolerances both set to 10^{-10}. At $t = 0$ I set $u = v = 0$ except for a small perturbation near $x = 0$. The solutions are plotted for $x > 0$ only, but I actually solved on $-L < x < L$ for L sufficiently large that the solution remains close to $u = v = 0$ near the domain boundaries $x = \pm L$ during the time period considered. The boundary conditions are $u = v = 0$ at $x = \pm L$; this avoids the difficulties posed by non-Dirichlet boundary conditions for nonlocal equations. The parameter values are $\delta = 1$, $\lambda_0 = 0.8$, and $\epsilon = 0.2$ with (a) $\omega_0 = 3.0$, $\omega_1 = -3.0$, $\lambda_1 = 2.8$; (b) $\omega_0 = 1.0$, $\omega_1 = 3.0$, $\lambda_1 = 2.8$; (c) $\omega_0 = 3.0$, $\omega_1 = -3.0$, $\lambda_1 = 1.0$; (d) $\omega_0 = 3.0$, $\omega_1 = -3.0$, $\lambda_1 = 0.08$. In (a)–(c) the solution is plotted for $105 \le t \le 135$; in (d) $t = 120$. By choosing L sufficiently large I deliberately avoid consideration of the longer term behavior after the spatiotemporal patterns spread over the whole domain. This is an important objective for future work: necessarily work such as that in the present paper must be done first. There are some results on long-term behavior following PTW generation on finite domains for reaction-diffusion models [40], but none (to my knowledge) for nonlocal models.*

of Brommer et al. work on voles in Finland [41]. The alternative process of predators invading a population of prey is more complex and has yet to be addressed in models with nonlocal dispersal, other than in numerical simulations. For reaction-diffusion

models it is known that the two processes actually select the same PTW solution close to a Hopf bifurcation in the kinetics [42]; however, there is no corresponding result for integrodifferential equation models.

4. Periodic traveling wave selection and stability for small ϵ. My basic approach in this paper is to calculate asymptotic expansions in ϵ for the various conditions in section 3, in order to determine how a small but nonzero value of ϵ affects PTW behavior, relative to the local dispersal limit of $\epsilon \to 0$. I consider the Gaussian kernel (2.2) and I fix $\delta = 4/\epsilon^2$; I comment on the case of the Laplace kernel (2.3) in section 7.

4.1. PTW existence. For the Gaussian kernel (2.2), (3.1) implies

$$\lambda_0 - \lambda_1 R^2 = \frac{4}{\epsilon^2} \left[1 - \frac{1}{\epsilon\sqrt{\pi}} \int_{s=-\infty}^{s=\infty} e^{-s^2/\epsilon^2} \cos \alpha s \, ds \right]$$

$$= \frac{4}{\epsilon^2} \left[1 - \frac{1}{\epsilon\sqrt{\pi}} \int_{s=-\infty}^{s=\infty} e^{-s^2/\epsilon^2} \left\{ 1 - \frac{1}{2}\alpha^2 s^2 + \frac{1}{24}\alpha^4 s^4 + \cdots \right\} ds \right]$$

$$\sim \frac{4}{\epsilon^2} \left[1 - \frac{1}{\epsilon\sqrt{\pi}} \left\{ \int_{s=-\infty}^{s=\infty} e^{-s^2/\epsilon^2} ds - \frac{1}{2}\alpha^2 \int_{s=-\infty}^{s=\infty} s^2 e^{-s^2/\epsilon^2} ds \right. \right.$$

$$\left. \left. + \frac{1}{24}\alpha^4 \int_{s=-\infty}^{s=\infty} s^4 e^{-s^2/\epsilon^2} ds + \cdots \right\} \right] \quad \text{using Watson's lemma}$$

(4.1) $$= \alpha^2 - \frac{1}{8}\epsilon^2\alpha^4 + O(\epsilon^4).$$

This relationship between PTW amplitude and wavenumber defines the PTW family. Note that the first two terms in the expansion (4.1) depend on the dispersal kernel only through its second and fourth moments.

4.2. PTW stability. Asymptotic expansions of the integrals in (3.2) can be obtained in a similar way. This gives the condition for PTW stability as

(4.2) $$\alpha^2 \left(3 + 2\omega_1^2/\lambda_1^2 \right) + \tfrac{1}{8}\epsilon^2\alpha^4 \left(3 + 4\omega_1^2/\lambda_1^2 \right) + O(\epsilon^4) < \lambda_0.$$

As expected, setting $\epsilon = 0$ in (4.2) gives the condition for PTW stability in a reaction-diffusion system of λ–ω type, which has been known since the 1970s (e.g., equation (41) in [8]).

4.3. Spreading speed. An asymptotic expansion of the moment generating function $M(.)$ of the Gaussian kernel (2.2) can again be found using Watson's lemma, giving

$$M(\eta) = \frac{1}{\epsilon\sqrt{\pi}} \int_{s=-\infty}^{s=\infty} e^{-s^2/\epsilon^2} e^{\eta s} \, ds \sim 1 + \frac{1}{4}\epsilon^2\eta^2 + \frac{1}{32}\epsilon^4\eta^4 + O(\epsilon^6).$$

Therefore

$$\left[\delta M(\eta) - \delta + \lambda_0 \right]/\eta \sim \lambda_0/\eta + \eta + \tfrac{1}{8}\epsilon^2\eta^3 + O(\epsilon^4)$$

whose minimum occurs at $\eta = \lambda_0^{1/2} - \frac{3}{16}\epsilon^2\lambda_0^{3/2} + O(\epsilon^4)$, giving

(4.3) $$c = 2\lambda_0^{1/2} + \tfrac{1}{8}\epsilon^2\lambda_0^{3/2} + O(\epsilon^4).$$

Again the first two terms in this expansion depend on the dispersal kernel only through its second and fourth moments.

4.4. PTW selection by a localized perturbation of $u = v = 0$. Substituting the expressions (4.3) for the spreading speed c and (4.1) for the PTW amplitude R into (3.3) gives the wavenumber of the PTW selected by localized perturbation of $u = v = 0$ as

$$(4.4a) \qquad\qquad \alpha = \alpha_0 + \epsilon^2 \alpha_1 + O(\epsilon^4),$$

$$(4.4b) \qquad \text{where } \alpha_0 = \lambda_0^{1/2} \left[(\lambda_1/\omega_1) - \text{sign}(\omega_1)\sqrt{1 + (\lambda_1/\omega_1)^2} \right]$$

$$(4.4c) \qquad \text{and } \alpha_1 = \frac{\alpha_0}{16} \cdot \frac{\alpha_0^3 + \lambda_0^{3/2}\lambda_1/\omega_1}{\alpha_0 - \lambda_0^{1/2}\lambda_1/\omega_1}.$$

Note that (3.3) actually gives a quadratic equation for α_0; the appropriate root has a sign opposite to that of ω_1.

4.5. Effects of nonlocal dispersal on wavenumber selection. My focus in this paper is to compare PTW generation by localized perturbation of $u = v = 0$ when $\epsilon = 0$ (local dispersal) and $\epsilon > 0$ (slightly nonlocal dispersal). Equation (4.3) shows that the speed of PTW spread is faster in the latter case—as expected, long-range dispersal accelerates the spreading speed. To investigate differences in the wavenumber of the selected PTW, it is convenient to write $\xi = \lambda_1/|\omega_1|$. Then

$$\alpha_1 = -\text{sign}(\omega_1) \cdot \left[\frac{\lambda_0^{3/2}}{16} \cdot \frac{\sqrt{1+\xi^2} - \xi}{\sqrt{1+\xi^2}} \right] \cdot Q(\xi),$$

$$\text{where } Q(\xi) = \left(\sqrt{1+\xi^2} - \xi \right)^3 - \xi$$

$$= \left(1+\xi^2\right)^{1/2}\left(1 + 4\xi^2\right) - 4\xi\left(1 + \xi^2\right)$$

$$= \frac{\left(1 + 8\xi^2 + 16\xi^4\right) - 16\xi^2(1 + \xi^2)}{\left(1+\xi^2\right)^{-1/2}\left(1 + 4\xi^2\right) + 4\xi}$$

$$= \frac{1 - 8\xi^2}{\left(1+\xi^2\right)^{-1/2}\left(1 + 4\xi^2\right) + 4\xi}.$$

Recall that the sign of α_0 is opposite to that of ω_1. Therefore α_1 has the same sign as α_0 if and only if $\xi < 1/\sqrt{8} \approx 0.354$. In that case a small degree of nonlocal dispersal increases the absolute value of the wavenumber of the selected PTW (and thus decreases its wavelength); for ξ above $1/\sqrt{8}$ the wavelength increases.

4.6. Effects of nonlocal dispersal on PTW stability. Another important consideration is how nonlocal dispersal affects the stability of the selected PTW. Substituting (4.4) into (4.2) gives a criterion for stability, but it is very complicated algebraically. To simplify it, I write $\alpha_0 = \text{sign}(\omega_1)\lambda_0^{1/2}\overline{\alpha}_0$, $\alpha_1 = \text{sign}(\omega_1)\lambda_0^{1/2}\overline{\alpha}_1$, $\epsilon = \lambda_0^{1/2}\overline{\epsilon}$, and as before $\xi = \lambda_1/|\omega_1|$. With these rescalings the stability criterion has no explicit dependence on λ_0 or on the sign of ω_1; its form is $\mathcal{F}_1(\xi) + \overline{\epsilon}^2\mathcal{F}_2(\xi) + O(\overline{\epsilon}^4) < 0$,

where

$$\mathcal{F}_1(\xi) = \left(\sqrt{1+\xi^2} - \xi\right)^2 (3\xi^2 + 2) - \xi^2,$$

$$\mathcal{F}_2(\xi) = \left(1+\xi^2\right)^{-1/2} (3\xi^2 + 2) \left[\left\{\left(1+\xi^2\right)^{1/2} - \xi\right\}^3 - \xi\right]$$

$$+ \left(3\xi^2 + 4\right) \left\{\left(1+\xi^2\right)^{1/2} - \xi\right\}^2.$$

Now

$$\mathcal{F}_1(\xi) < 0 \Leftrightarrow 2\xi\left(3\xi^2 + 2\right)\left(1+\xi^2\right)^{1/2} > \left(1+2\xi^2\right)\left(3\xi^2 + 2\right) - \xi^2.$$

Since both sides of this inequality are positive, one can square them, which gives $\mathcal{C}(\xi^2) > 0$, where $\mathcal{C}$ is a cubic polynomial with a positive leading coefficient and with a unique real positive root, which can easily be calculated numerically as $0.871\ldots$. Therefore to leading order in ϵ, the selected PTW is stable $\Leftrightarrow \xi > \sqrt{0.871\ldots} \approx 0.933$.

Turning now to $\mathcal{F}_2(\xi)$, this simplifies to

$$\mathcal{F}_2(\xi) = 2(1+\xi^2)^{1/2} \left[\left(9\xi^4 + 11\xi^2 + 3\right) - \xi\left(9\xi^2 + 8\right)\left(1+\xi^2\right)^{1/2}\right]$$

$$= \frac{2(1+\xi^2)^{1/2}\left(9 + 2\xi^2 - 33\xi^4 - 27\xi^6\right)}{\left(9\xi^4 + 11\xi^2 + 3\right) + \xi\left(9\xi^2 + 8\right)\left(1+\xi^2\right)^{1/2}}.$$

The numerator in this expression is a cubic polynomial in ξ^2 with a unique real positive root at $\xi^2 = 0.467\ldots$, implying that $\mathcal{F}_2(\xi) < 0 \Leftrightarrow \xi > \sqrt{0.467\ldots} = 0.683\ldots$. The key implication of this is that $\mathcal{F}_2(\xi) < 0$ whenever $\mathcal{F}_1(\xi) < 0$, so that a small degree of nonlocality in dispersal always increases the region of parameter space in which the selected PTW is stable.

5. Absolute stability of the periodic traveling wave selected by a localized perturbation of $u = v = 0$. In spatiotemporal systems, unstable solutions subdivide into those that are "absolutely unstable" and those that are "convectively unstable" but "absolutely stable" (see [43] for a detailed review). The distinction lies in the spatiotemporal behavior of small perturbations. In the convectively unstable case all growing perturbations move while they are growing and actually decay at their original location. In contrast, absolute instability is defined by the growth of a small perturbation at its point of application. For PTWs generated by a localized perturbation of an unstable steady state, the two types of instability lead to very different spatiotemporal behavior. When the PTW is convectively unstable, one sees bands of alternating left- and right-moving PTWs separated by sharp transitions known as sources and sinks [44, 45, 46]. The change from convective to absolute instability in the selected PTW leads to a single band of PTWs followed by more comprehensive disorder (Figure 3.1(c)). Another change occurs when the selected PTW becomes absolutely unstable not just in a stationary frame of reference but also in a frame moving with the spreading speed. Then spatiotemporal disorder arises immediately, without a band of PTWs (Figure 3.1(d)).

To my knowledge there are no results on the absolute stability of solutions of integrodifferential equations, but I will show that it is possible to determine the absolute stability of the PTW selected by a localized perturbation of $u = v = 0$ when the parameter ϵ is small. I begin by rewriting (2.1) in terms of the amplitude $r = \sqrt{u^2 + v^2}$

and phase $\theta = \tan^{-1}(v/u)$:

(5.1a) $\qquad \dfrac{\partial r}{\partial t} = \delta \displaystyle\int_{y=-\infty}^{y=+\infty} K(y-x) r(y) \cos\big[\theta(y)-\theta(x)\big]\,dy + r\lambda(r) - r\,,$

(5.1b) $\qquad \dfrac{\partial \theta}{\partial t} = \delta \displaystyle\int_{y=-\infty}^{y=+\infty} K(y-x) \dfrac{r(y)}{r(x)} \sin\big[\theta(y)-\theta(x)\big]\,dy + \omega(r)\,.$

The advantage of this formulation is that PTW solutions have a particularly simple form: $r = R$, $\theta = \big(\omega_0 + \omega_1 R^2\big)t \pm \alpha x$. As with stability, the investigation of absolute stability begins by linearizing (5.1) about this PTW and looking for solutions proportional to $e^{\nu x + \Lambda t}$. The criterion for nontrivial solutions of this type (the "dispersion relation") is

(5.2) $\qquad \mathcal{D}(\Lambda, \nu) \equiv (\Lambda - A)(\Lambda - D) - BC = 0\,,$

$\qquad$ where $A = \lambda_0 - 3\lambda_1 R^2 + \nu^2 - \alpha^2 + \tfrac{1}{8}\epsilon^2\big(\alpha^4 + \nu^4 - 6\alpha^2\nu^2\big) + O(\epsilon^4)\,,$

$\qquad\qquad B = -2R\alpha\nu + \tfrac{1}{2}\epsilon^2\alpha\nu(\alpha^2 - \nu^2)R + O(\epsilon^4)\,,$

$\qquad\qquad C = 2\omega_1 R + 2\alpha\nu/R - \tfrac{1}{2}\epsilon^2\alpha\nu\big(\alpha^2 - \nu^2\big)/R + O(\epsilon^4)\,,$

$\qquad\qquad D = \lambda_0 - \lambda_1 R^2 + \nu^2 - \alpha^2 + \tfrac{1}{8}\epsilon^2\big(\alpha^4 + \nu^4 - 6\alpha^2\nu^2\big) + O(\epsilon^4)\,.$

PTW stability depends on the sign of $\mathrm{Re}\,\Lambda$ in solutions of (5.2) with $\mathrm{Re}\,\nu = 0$, but for absolute stability, one must consider ν with nonzero real and imaginary parts. For spatially uniform solutions of certain classes of PDE, absolute stability is determined by repeated roots for ν of $\mathcal{D}(\Lambda, \nu) = 0$, i.e., simultaneous roots of $\mathcal{D}(\Lambda, \nu) = (\partial/\partial\nu)\mathcal{D}(\Lambda, \nu) = 0$. Specifically, denote the repeated roots by $\nu_1, \nu_2, \ldots, \nu_N$, where $\mathrm{Re}\,\nu_i \geq \mathrm{Re}\,\nu_{i+1}$, and suppose that the PDE is such that on a finite domain with separated boundary conditions, n_L conditions are required on the left-hand boundary, and n_R on the right ($n_L + n_R = N$). Then (Λ, ν) pairs for which $\mathcal{D}(\Lambda, \nu) = (\partial/\partial\nu)\mathcal{D}(\Lambda, \nu) = 0$ and for which the repeated roots for ν are ν_{n_L} and ν_{n_L+1} are known as "saddle points satisfying the pinching condition" [47, 48] or as "branch points of the absolute spectrum" [49]. The PTW is absolutely stable if and only if all such pairs have $\mathrm{Re}\,\Lambda \leq 0$. (See [49] for a precise statement and for the required technical conditions.) Note that the two distinct terminologies reflect two quite different approaches to considering absolute stability, one developed in the physics literature, initially by Richard Briggs in the 1960s [50], and the other developed more recently by Björn Sandstede and Arnd Scheel [49].

$\qquad$ Although the theory underlying the above remarks is rather complicated, its practical implementation is relatively straightforward. One simply has to study (usually numerically) roots for ν of the polynomial $\mathcal{D}(\Lambda, \nu) = 0$. However, it depends fundamentally on $\mathcal{D}(\Lambda, \nu) = (\partial/\partial\nu)\mathcal{D}(\Lambda, \nu) = 0$ having a finite number of roots. This is guaranteed for a partial differential equation since $\mathcal{D}$ is then a polynomial, but for an integrodifferential equation $\mathcal{D}$ can have an infinite number of repeated roots for ν, so that n_L and n_R are not defined. However, asymptotic expansion for small ϵ restores the polynomial form for $\mathcal{D}$, enabling absolute stability to be determined. Neglecting terms that are $O(\epsilon^4)$ and writing $\overline{\nu} = \lambda_0^{1/2}\nu$, $\overline{\epsilon} = \lambda_0^{1/2}\epsilon$, and $\overline{\Lambda} = \Lambda/\lambda_0$ gives the dispersion relation as

(5.3) $\qquad \mathcal{D}_1(\overline{\Lambda}, \overline{\nu}) \equiv \overline{\Lambda}^2 - \big[\mathcal{P}_2(\overline{\nu}) + \overline{\epsilon}^2\mathcal{P}_4(\overline{\nu})\big]\overline{\Lambda} + \big[\mathcal{Q}_4(\overline{\nu}) + \overline{\epsilon}^2\mathcal{Q}_8(\overline{\nu})\big] = 0,$

where $\mathcal{P}_2$, $\mathcal{P}_4$, $\mathcal{Q}_4$, and $\mathcal{Q}_8$ are polynomials of degree 2, 4, 4, and 8 (respectively) in $\bar{\nu}$; their algebraic forms are rather complicated and are omitted for brevity. The various rescalings result in there being no explicit dependence on λ_0: thus the coefficients of $\bar{\nu}$ in the $\mathcal{P}_i$'s and $\mathcal{Q}_i$'s are functions of ξ only. Ordering the roots of (5.3) for $\bar{\nu}$ by real part as above ($\operatorname{Re}\bar{\nu}_i > \operatorname{Re}\bar{\nu}_{i+1}$), the transition from convective to absolute stability occurs when $\bar{\nu}_4 = \bar{\nu}_5$ with $\operatorname{Re}\bar{\Lambda} = 0$.

When $\epsilon = 0$ the dispersion relation (5.3) reduces to a quartic polynomial in $\bar{\nu}$, which has been studied in previous work on the absolute stability of PTWs in reaction-diffusion equations of λ–ω type [17]. I denote the four roots of this quartic by $\bar{\nu}_1^{\epsilon=0}, \ldots, \bar{\nu}_4^{\epsilon=0}$, again with $\operatorname{Re}\bar{\nu}_i^{\epsilon=0} \geq \operatorname{Re}\bar{\nu}_{i+1}^{\epsilon=0}$. It is important to consider how the $\bar{\nu}_i$'s are related to the $\bar{\nu}_i^{\epsilon=0}$'s. Clearly four of the $\bar{\nu}_i$'s are small perturbations of the $\bar{\nu}_i^{\epsilon=0}$'s; the other four approach infinity as $\bar{\epsilon} \to 0$. To investigate this latter group in more detail, I note that when $|\bar{\nu}|$ is large the dominant terms in $\mathcal{Q}_4(\bar{\nu})$ and $\mathcal{Q}_8(\bar{\nu})$ are $\bar{\nu}^4$ and $\frac{1}{8}\bar{\nu}^8$, respectively. These must balance, so that $\frac{1}{8}\bar{\epsilon}^4\bar{\nu}^8 + \bar{\nu}^4 = 0$ to leading order, implying that the roots approach infinity as $\bar{\epsilon} \to 0$ with $\bar{\nu}^4 \sim -8/\bar{\epsilon}^4 \Rightarrow \bar{\nu} \sim 2^{1/4}(1 \pm i)/\bar{\epsilon}$, and $2^{1/4}(-1 \pm i)/\bar{\epsilon}$. Therefore these roots are respectively $\bar{\nu}_1$, $\bar{\nu}_2$, $\bar{\nu}_7$, and $\bar{\nu}_8$. It follows that $\bar{\nu}_4$ and $\bar{\nu}_5$ are small perturbations of $\bar{\nu}_2^{\epsilon=0}$ and $\bar{\nu}_3^{\epsilon=0}$, with the transition from convective to absolute stability occurring when these roots are equal with $\operatorname{Re}\bar{\Lambda} = 0$.

Investigation of the roots for $\bar{\nu}^{\epsilon=0}$ was presented previously in [17]. Briefly, elimination of $\bar{\Lambda}$ between $\mathcal{D}_1|_{\bar{\epsilon}=0} = 0$ and $(\partial/\partial\bar{\nu})\mathcal{D}_1|_{\bar{\epsilon}=0} = 0$ gives a quartic polynomial in $\bar{\nu}^{\epsilon=0}$, with coefficients depending on ξ. For any given ξ this polynomial can easily be solved numerically, and each of the four roots can be substituted back into $(\partial/\partial\bar{\nu})\mathcal{D}_1|_{\bar{\epsilon}=0} = 0$ to give the corresponding values of $\bar{\Lambda}$. By tracking these roots for $\bar{\nu}$ and $\bar{\Lambda}$ as ξ is varied, it is straightforward to calculate critical values of ξ at which $\operatorname{Re}\bar{\Lambda}$ changes sign. At such points, the (pure imaginary) value of $\bar{\Lambda}$ can be substituted back into $\mathcal{D}_1|_{\bar{\epsilon}=0} = 0$, which can then be solved (numerically); this will recover the repeated roots for $\bar{\nu}$ and will give two additional roots. This procedure shows that there is one case in which the repeated roots are $\bar{\nu}_2^{\epsilon=0} = \bar{\nu}_3^{\epsilon=0}$, corresponding to a change in absolute stability, namely,

$$(5.4) \qquad \xi \approx 0.661 \qquad \bar{\nu}_2^{\epsilon=0} = \bar{\nu}_3^{\epsilon=0} \approx -0.256 + 0.564i \qquad \bar{\Lambda} \approx 0.561i\,.$$

Details of this procedure are given in [17].

The critical case (5.4) provides a starting point for calculating the transition point when $\bar{\epsilon} > 0$. I fix $\bar{\Lambda}$ to be pure imaginary in (5.3), with $\bar{\epsilon}$ positive but very small, and solve $\mathcal{D}_1 = \partial\mathcal{D}_1/\partial\bar{\nu} = 0$ numerically using (5.4) as an "initial guess." I then gradually increase $\bar{\epsilon}$, on each occasion using the solution for the previous value of $\bar{\epsilon}$ as an "initial guess." The results of this calculation are illustrated in Figure 5.1(a), in which the threshold value of ξ for absolute stability is plotted against $\bar{\epsilon}$.

Absolute stability in a frame of reference moving with the spreading speed can be calculated in a directly analogous way. In this case the dispersion relation is

$$\left(\bar{\Lambda} - \bar{c}\,\bar{\nu}\right)^2 - \mathcal{P}\left(\bar{\Lambda} - \bar{c}\,\bar{\nu}\right) + \mathcal{Q} = 0,$$

where $O(\bar{\epsilon}^4)$ terms have been neglected. Here $\bar{c} = c/\lambda_0^{1/2}$ and c is the spreading speed, given in (4.3); thus $\bar{c} = 2 + \frac{1}{8}\bar{\epsilon}^2$. For $\bar{\epsilon} = 0$ the transition from convective to absolute instability of the PTW generated by a localized perturbation of $u = v = 0$ occurs at $\xi \approx 0.0534$[1] and again the critical value of ξ increases with $\bar{\epsilon}$, as illustrated

---

[1]The corresponding spatial and temporal eigenvalues are $\bar{\nu} \approx -1.082 + 0.999i$ and $\bar{\Lambda} \approx 3.41i$.
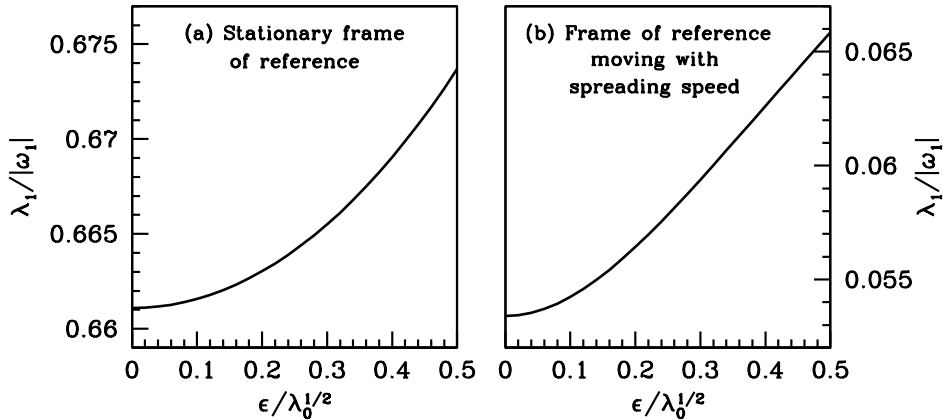
FIG. 5.1. *The threshold value of the parameter $\xi = \lambda_1/|\omega_1|$ for absolute stability of the PTW generated by a localized perturbation of $u = v = 0$ in the λ–ω integrodifferential equation model* (2.1), *as a function of the parameter $\bar{\epsilon} = \epsilon/\lambda_0^{1/2}$ in the dispersal kernel. Part* (a) *shows the critical value for absolute stability in a stationary frame of reference; this is the division between "source-sink" behavior* [44, 45, 46] *and a band of PTWs followed by more comprehensive disorder. Part* (b) *shows the critical value for absolute stability in a frame of reference moving with the spreading speed; for ξ below this value there is spatiotemporal disorder without a band of PTWs.*

in Figure 5.1(b). For ξ below this value, there is no band of PTWs but rather an immediate onset of spatiotemporal disorder.

Note that, as in section 4, the results derived in this section depend on the dispersal kernel only through its second and fourth moments.

6. Application to a predator-prey model. The λ–ω equations (2.1) are not a model for any particular biological or physical system; rather their significance is as the normal form of models for real systems close to a (standard supercritical) Hopf bifurcation. As an illustration of applying the results that I have derived for (2.1), I consider the predator-prey model given by the Rosenzweig–MacArthur kinetics [51] with nonlocal dispersal:

(6.1a)

$$\boxed{\text{predators}}\ \frac{\partial p}{\partial t} = \tilde{\delta}\overbrace{\left[\int_{y=-\infty}^{y=\infty} K(x-y)p(y,t)dy - p\right]}^{\text{dispersal}} + \overbrace{(\tilde{C}/\tilde{B})hp/(1+\tilde{C}h)}^{\substack{\text{benefit from}\\\text{predation}}} - \overbrace{p/\tilde{A}\tilde{B}}^{\text{death}},$$

(6.1b)

$$\boxed{\text{prey}}\ \frac{\partial h}{\partial t} = \tilde{\delta}\underbrace{\left[\int_{y=-\infty}^{y=+\infty} K(x-y)h(y,t)dy - h\right]}_{\text{dispersal}} + \underbrace{h(1-h)}_{\substack{\text{intrinsic}\\\text{birth \& death}}} - \underbrace{\frac{\tilde{C}ph}{1+\tilde{C}h}}_{\text{predation}}.$$

These equations are nondimensional with $p(x,t)$ and $h(x,t)$ denoting predator and prey densities at space point x and time t. $\tilde{A}$, $\tilde{B}$, $\tilde{C}$, and $\tilde{\delta}$ are positive constants. The prey consumption rate per predator is taken to be an increasing saturating function of prey density with Holling type II form: $\tilde{C} > 0$ reflects how quickly the function saturates. Parameters $\tilde{A} > 0$ and $\tilde{B} > 0$ are dimensionless combinations of the birth and death rates. Equations (6.1) have a unique coexistence steady state which has a (standard supercritical) Hopf bifurcation at $\tilde{C} = (\tilde{A}+1)/(\tilde{A}-1)$. Treating $\tilde{C}$ as the
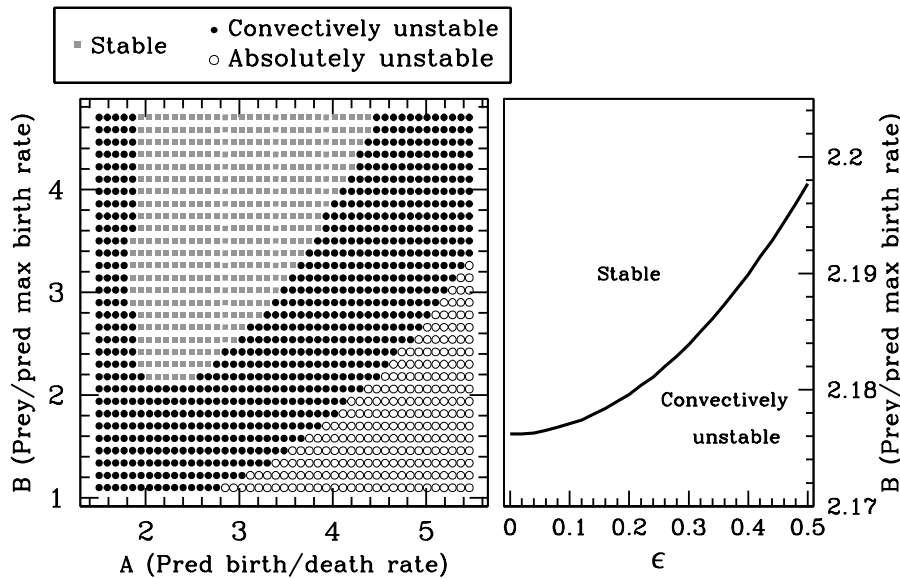
FIG. 6.1. *The stability of the PTW generated by a localized perturbation of the coexistence steady state in* (6.1) *for* $\tilde{C}$ *a little above the Hopf bifurcation value* $(\tilde{A}+1)/(\tilde{A}-1)$, *as a function of the parameters* $\tilde{A}$ *and* $\tilde{B}$. *The Gaussian kernel* (2.2) *is used for dispersal, but the corresponding pictures for the Laplace kernel* (2.3) *are very similar. In the left-hand panel I fixed* $\epsilon = 0.2$ *and considered a regular grid of* $(\tilde{A}, \tilde{B})$ *points. For each point I calculated* λ_0, λ_1, *and* ω_1 *using* (6.2), *which gives* $\xi = \lambda_1/|\omega_1|$ *and* $\bar{\epsilon} = \lambda_0^{1/2}\epsilon$. *The calculations in the main body of the text then enable determination of the stability and absolute stability of the selected PTW. In the right-hand panel I used a similar approach to determine the boundary in the* ϵ–$\tilde{B}$ *parameter plane between stability and (convective) instability for* $\tilde{A} = 2.5$. *In both parts of the figure,* $\tilde{C}$ *is set to* $1.2(\tilde{A}+1)/(\tilde{A}-1)$.

bifurcation parameter, the standard process of reduction to normal form [33, 31, 32] gives (2.1) to leading order, with

$$(6.2a) \qquad \lambda_0 = \frac{(\tilde{A}-1)\tilde{C} - (\tilde{A}+1)}{2\tilde{A}(\tilde{A}+1)}, \qquad \lambda_1 = \frac{\tilde{A}+1}{4\tilde{A}},$$

$$(6.2b) \qquad \omega_0 = \left(\frac{\tilde{A}-1}{\tilde{A}\tilde{B}(\tilde{A}+1)}\right)^{1/2} + \frac{\left[(\tilde{A}-1)\tilde{C} - (\tilde{A}+1)\right](\tilde{A}-1)^{1/2}}{2\tilde{A}^{3/2}(\tilde{A}+1)^{3/2}\tilde{B}^{1/2}},$$

$$(6.2c) \qquad \omega_1 = \frac{(\tilde{A}+1)^{1/2}\left(2\tilde{A}^2 + 5\tilde{A}\tilde{B} - \tilde{A}^5\tilde{B} - \tilde{A}^4 - 4\tilde{A}^3\tilde{B} - 4\tilde{A}^2\tilde{B}^2 - 1\right)}{24[\tilde{A}^7(\tilde{A}-1)\tilde{B}^3]^{1/2}}.$$

(See [18, 16] for details of the calculations for the specific case of the Rosenzweig–MacArthur kinetics, including Maple worksheets.)

The expressions (6.2) enable $\xi = \lambda_1/|\omega_1|$ to be calculated in terms of $\tilde{A}$ and $\tilde{B}$. From this, one can determine the stability and absolute stability of the PTW selected by a localized perturbation of the coexistence steady state, using the results in sections 4 and 5. This is illustrated in Figure 6.1, which also shows the effect of changing the kernel parameter ϵ on this parameter plane. Such a division of the $\tilde{A}$–$\tilde{B}$ parameter plane makes it possible to predict the type of spatiotemporal dynamics expected following a localized perturbation of the coexistence steady state.
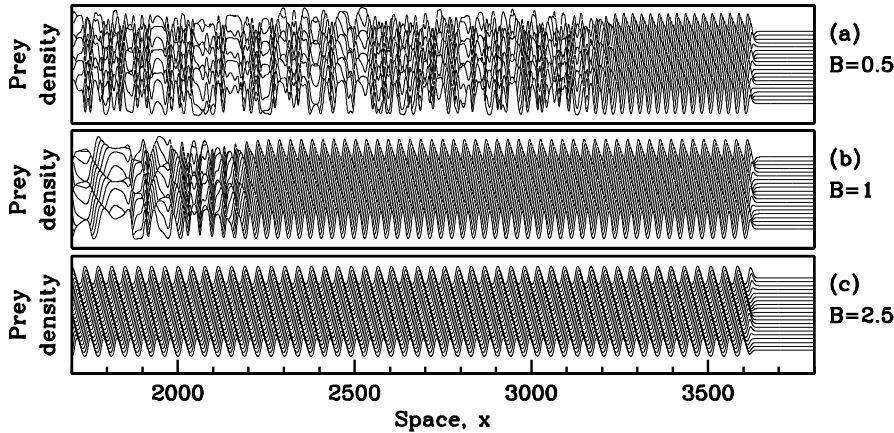
Fig. 6.2. *Examples of PTW generation by a localized perturbation of the coexistence steady state in the predator-prey model* (6.1). *In* (a) *and* (b) *the selected PTW is unstable, and there is a band of PTWs followed by spatiotemporal disorder; in* (c) *the selected PTW is stable and persists. The equations were solved numerically as described in the legend to Figure* 3.1; *the spatial grid spacing* δx *was set to* 0.5. *The perturbation to the coexistence steady state was applied at the center* $x = 0$ *of a large spatial domain. As in Figure* 3.1 *I used Dirichlet boundary conditions and I stopped the simulation before the PTWs reached the boundaries of the domain. I used the Laplace kernel* (2.3) *with* $\epsilon_l = 0.5$; *the parameter values are* $\tilde{A} = 2$, $\tilde{C} = 3.6$, $\tilde{\delta} = 1$, *and* (a) $\tilde{B} = 0.5$, (b) $\tilde{B} = 1.0$, (c) $\tilde{B} = 2.5$. *In all three parts of the figure, the solution is plotted for* $18800 \le t \le 18880$.

Figure 6.2 shows numerical simulations of these dynamics. For small $\tilde{B}$, there is a relatively narrow band of PTWs followed by spatiotemporal disorder (Figure 6.2(a)). As $\tilde{B}$ in increased (with other parameters fixed) the band of PTWs becomes wider (Figure 6.2(b)) and for sufficiently large $\tilde{B}$ the selected PTW is stable and persists (Figure 6.2(c)).

7. Discussion. The detection of PTW behavior in spatiotemporal datasets from ecology demands a detailed mathematical understanding of PTW solutions of ecologically realistic models. For many species such models must include nonlocal dispersal. This paper is the third in a series studying PTWs in the integrodifferential equations that arise when one uses a convolution-based representation of dispersal. I have focused on the generation of PTWs by a localized perturbation of an unstable steady state, showing how nonlocality in dispersal affects PTW selection, stability, and absolute stability.

I have restricted attention to the Gaussian dispersal kernel, but conditions for existence and stability of PTWs are also known for the Laplace kernel (2.3) [24], as are results on PTW selection by localized perturbation of an unstable steady state [25]. All of the calculations in this paper can be repeated for the Laplace kernel. The appropriate choice for δ is then $1/\epsilon_l^2$, and if one uses this and redefines $\bar{\epsilon} = \epsilon_l / \left(\lambda_0^{1/2} \sqrt{8} \right)$, then the conditions on ξ for stability and absolute stability of the selected PTW are exactly the same as for the Gaussian kernel. To explain this, it is convenient to denote by M_2 and M_4 the second and fourth moments of the dispersal kernel. Then the key players in the calculations in sections 4 and 5 are δM_2 and $\bar{\epsilon}^2 \delta M_4$, and appropriate choices for δ and $\bar{\epsilon}$ (given above) make these the same for the Laplace kernel as for the Gaussian kernel. This would also be true for any other (thin-tailed) kernel, however, the key ingredient of a condition for PTW stability is then missing—this is only known for the two kernels that I have considered.
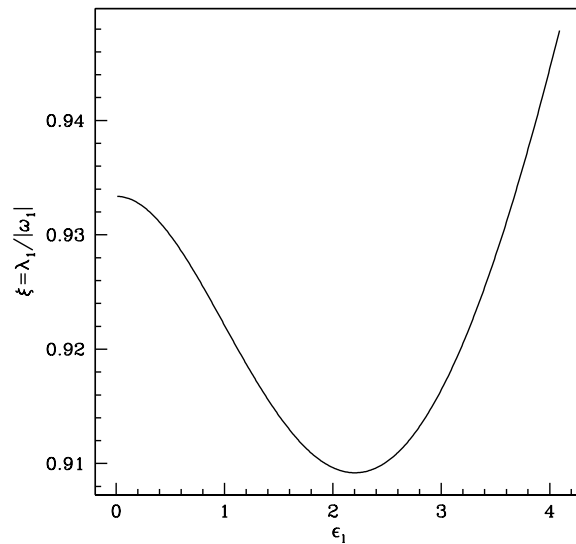
FIG. 7.1. *An example of numerical calculations of the critical value of $\xi = \lambda_1/|\omega_1|$ above which the PTW generated by a localized perturbation of an unstable steady state is stable. I use the Laplace kernel (2.3) and consider large values of ϵ_l: my analytical results are valid only for sufficiently small ϵ_l. The parameters are $\delta = 1$ and $\lambda_0 = 0.1$; the numerical procedure is outlined in the main text.*

All of my results concern behavior when the degree of nonlocality in dispersal is small, meaning that ϵ (or ϵ_l) is small. Analytical investigation of behavior for larger ϵ (or ϵ_l) is a much harder problem, but a numerical study is possible. Figure 7.1 shows one example of numerical results. I solved (3.1), (3.3), (3.4) numerically to calculate the wavenumber of the PTW selected by a localized perturbation of the steady state; in this case I used the Laplace kernel. Substituting this into (3.2) enables numerical calculation of PTW stability, and I repeated this process for different values of ξ in order to determine the critical ξ giving a change in stability. My analytical calculations show that for small ϵ_l this critical ξ will decrease as ϵ_l increases, and this is confirmed by the numerical calculations illustrated in the figure. However, for larger ϵ_l (above about 2.1) the trend reverses and the critical ξ increases with ϵ_l. This argues persuasively for the importance of detailed investigation of PTW generation when dispersal is significantly nonlocal.

Integrodifferential equations are certainly not the only class of ecological model that includes a representation of nonlocal dispersal. Integrodifference equations are also in widespread use, as are cellular automata and agent-based models incorporating long-range movement. The spatial and/or temporal discreteness in these models makes the study of PTWs particularly challenging, and thus integrodifferential equations are a natural starting point for investigating the role of nonlocal dispersal in PTW behavior.

I have focused on PTW generation by a localized perturbation of an unstable steady state because it is the best studied generation mechanism in models with local dispersal (e.g., [11, 9, 10]). However, other features of spatiotemporal systems can generate PTW behavior, including heterogeneous habitats [19, 5, 13] and hostile habitat boundaries [16, 14]. Neither of these has been studied for models with nonlocal dispersal, and this is a natural area for future work. Once basic results on PTW selection by these mechanisms in integrodifferential equation models have been obtained,

the approach of the present paper could be used to make a comparison between the selected PTWs when dispersal is local and when it has a small nonlocal component.

REFERENCES

[1] R. A. Ims, J.-A. Henden, and S. T. Killengreen, *Collapsing population cycles,* Trends Ecol. Evol., 23 (2008), pp. 79–86.

[2] K. L. Kausrud, A. Mysterud, H. Steen, J. O. Vik, E. Østbye, B. Cazelles, E. Framstad, A. M. Eikeset, I. Mysterud, T. Solhoy, and N. C. Stenseth, *Linking climate change to lemming cycles,* Nature, 456 (2008), pp. 93—97.

[3] S. M. Bierman, J. P. Fairbairn, S. J. Petty, D. A. Elston, D. Tidhar, and X. Lambin, *Changes over time in the spatiotemporal dynamics of cyclic populations of field voles (Microtus agrestis L.),* Am. Nat., 167 (2006), pp. 583–590.

[4] K. Berthier, S. Piry, J. F. Cosson, P. Giraudoux, J. C. Foltête, R. Defaut, D. Truchetet, and X. Lambin, *Dispersal, landscape and travelling waves in cyclic vole populations,* Ecol. Lett., 17 (2014), pp. 53–64.

[5] D. M. Johnson, O. N. Bjørnstad, and A. M. Liebhold, *Landscape mosaic induces traveling waves of insect outbreaks,* Oecologia, 148 (2006), pp. 51–60.

[6] R. Moss, D. A. Elston, and A. Watson, *Spatial asynchrony and demographic travelling waves during red grouse population cycles,* Ecology, 81 (2000), pp. 981–989.

[7] J. A. Sherratt and M. J. Smith, *Periodic travelling waves in cyclic populations: Field studies and reaction-diffusion models,* J. R. Soc. Interface, 5 (2008), pp. 483–505.

[8] N. Kopell and L. N. Howard, *Plane wave solutions to reaction-diffusion equations,* Stud. Appl. Math., 52 (1973), pp. 291–328.

[9] J. A. Sherratt, *Irregular wakes in reaction-diffusion waves,* Phys. D, 70 (1994), pp. 370–382.

[10] S. V. Petrovskii, M. E. Vinogradov, and A. Y. Morozov, *Spatial-temporal dynamics of a localized populational burst in a distributed prey-predator system,* Okeanologiya, 38 (1998), pp. 881–890.

[11] J. A. Sherratt, *On the evolution of periodic plane waves in reaction-diffusion equations of λ–ω type,* SIAM J. Appl. Math., 54 (1994), pp. 1374–1385.

[12] S. M. Merchant and W. Nagata, *Wave train selection behind invasion fronts in reaction-diffusion predator-prey models,* Phys. D, 239 (2010), pp. 1670–1680.

[13] A. L. Kay and J. A. Sherratt, *Spatial noise stabilizes periodic wave patterns in oscillatory systems on finite domains,* SIAM J. Appl. Math., 61 (2000), pp. 1013–1041.

[14] M. Sieber, H. Malchow, and S. V. Petrovskii, *Noise-induced suppression of periodic travelling waves in oscillatory reaction-diffusion systems,* Proc. R. Soc. Lond. A, 466 (2010), pp. 1903–1917.

[15] S. R. Dunbar, *Traveling waves in diffusive predator-prey equations: periodic orbits and point-to-periodic heteroclinic orbits,* SIAM J. Appl. Math., 46 (1986), pp. 1057–1078.

[16] J. A. Sherratt, X. Lambin, and T. N. Sherratt, *The effects of the size and shape of landscape features on the formation of traveling waves in cyclic populations,* Am. Nat., 162 (2003), pp. 503–513.

[17] M. J. Smith, J. D. M. Rademacher, and J. A. Sherratt, *Absolute stability of wavetrains can explain spatiotemporal dynamics in reaction-diffusion systems of lambda-omega type,* SIAM J. Appl. Dyn. Syst., 8 (2009), pp. 1136–1159.

[18] J. A. Sherratt, *Periodic travelling waves in cyclic predator-prey systems,* Ecol. Lett., 4 (2001), pp. 30–37.

[19] D. M. Johnson, O. N. Bjørnstad, and A. M. Liebhold, *Landscape geometry and travelling waves in the larch budmoth,* Ecol. Lett., 7 (2004), pp. 967–974.

[20] R. S. Cantrell and C. Cosner, *Spatial Ecology Via Reaction-Diffusion Equations,* Wiley, Chichester, UK, 2003.

[21] J. M. Bullock, L. Mallada González, R. Tamme, L. Götzenberger, S. M. White, M. Pärtel, and D. A. Hooftman, *A synthesis of empirical plant dispersal kernels,* J. Ecol., 105 (2017), pp. 6–19.

[22] Z. Fric and M. Konvicka, *Dispersal kernels of butterflies: power-law functions are invariant to marking frequency,* Basic Appl. Ecol., 8 (2007), pp. 377–386.

[23] A. W. Byrne, J. L. Quinn, J. J. O'Keeffe, S. Green, D. P. Sleeman, S. W. Martin, and J. Davenport, *Large-scale movements in European badgers: has the tail of the movement kernel been underestimated?* J. Anim. Ecol., 83 (2014), pp. 991–1001.

[24] J. A. Sherratt, *Periodic travelling waves in integrodifferential equations for nonlocal dispersal,* SIAM J. Appl. Dyn. Syst., 13 (2014), pp. 1517–1541.

[25] J. A. Sherratt, *Invasion generates periodic travelling waves (wavetrains) in predator-prey models with nonlocal dispersal,* SIAM J. Appl. Math., 76 (2016), pp. 293–313.

[26] C. Hauzy, F. D. Hulot, and A. Gins, *Intra and interspecific density-dependent dispersal in an aquatic prey–predator system,* J. Anim. Ecol. 76 (2007), pp. 552–558.

[27] M. J. Brandt and X. Lambin, *Movement patterns of a specialist predator, the weasel Mustela nivalis exploiting asynchronous cyclic field vole Microtus agrestis populations,* Acta Theriol., 52 (2007), pp. 13–25.

[28] E. A. Wieters, S. D. Gaines, S. A. Navarrete, C. A. Blanchette, and B. A. Menge, *Scales of dispersal and the biogeography of marine predator-prey interactions,* Am. Nat., 171 (2008), pp. 405–417.

[29] Y. Kuramoto, *Scaling behavior of turbulent oscillators with non-local interaction,* Prog. Theor. Phys., 94 (1995), pp. 321–330.

[30] D. Tanaka and Y. Kuramoto, *Complex Ginzburg-Landau equation with nonlocal coupling,* Phys. Rev. E, 68 (2003), 026219.

[31] V. García-Morales, R. W. Hölzel, and K. Krischer, *Coherent structures emerging from turbulence in the nonlocal complex Ginzburg-Landau equation,* Phys. Rev. E, 78 (2008), 026215.

[32] V. García-Morales and K. Krischer, *Nonlocal complex Ginzburg-Landau equation for electrochemical systems,* Phys. Rev. Lett., 100 (2008), 054101.

[33] Y. A. Kuznetsov, *Elements of Applied Bifurcation Theory,* Springer-Verlag, New York, 2004.

[34] J. Medlock and M. Kot, *Spreading disease: integro-differential equations old and new,* Math. Biosci., 184 (2003), pp. 201–222.

[35] F. Lutscher, E. Pachepsky, and M.A. Lewis *The effect of dispersal patterns on stream populations,* SIAM J. Appl. Math., 65 (2005), pp. 1305–1327.

[36] M. A. Gilbert, S. M. White, J. M. Bullock, and E. A. Gaffney, *Spreading speeds for stage structured plant populations in fragmented landscapes,* J. Theoret. Biol., 349 (2014), pp. 135–149.

[37] L. Eigentler and J. A. Sherratt *Analysis of a model for banded vegetation patterns in semi-arid environments with nonlocal dispersal,* J. Math. Biol., 17 (2018), pp. 1–25.

[38] G.-B. Zhang, W.-T. Li, and Z.-C. Wang, *Spreading speeds and traveling waves for nonlocal dispersal equations with degenerate monostable nonlinearity,* J. Differential Equations, 252 (2012), pp. 5096–5124.

[39] R. Weiner, B. A. Schmitt, and H. Podhaisky, *ROWMAP – a ROW-code with Krylov techniques for large stiff ODEs,* Appl. Numer. Math., 25 (1997), pp. 303–319.

[40] A. L. Kay and J. A. Sherratt, *On the persistence of spatiotemporal oscillations generated by invasion,* IMA J. Appl. Math., 63 (1999), pp. 199–216.

[41] J. E. Brommer, H. Pietiäinen, K. Ahola, P. Karell, T. Karstinen, and H. Kolunen, *The return of the vole cycle in southern Finland refutes the generality of the loss of cycles through 'climatic forcing',* Glob. Change Biol., 16 (2010), pp. 577–586.

[42] J. A. Sherratt, *Generation of periodic travelling waves in cyclic populations by hostile boundaries,* Proc. R. Soc. Lond. A, 469 (2013), 20120756.

[43] J. A. Sherratt, A.S. Dagbovie, and F.M. Hilker, *A mathematical biologist's guide to absolute and convective instability,* Bull. Math. Biol., 76 (2014), pp. 1–26.

[44] M. van Hecke, C. Storm, and W. van Saarloos, *Sources, sinks and wavenumber selection in coupled CGL equations and experimental implications for counter-propagating wave systems,* Phys. A, 134 (1999), pp. 1–47.

[45] B. Sandstede and A. Scheel, *Defects in oscillatory media: toward a classification,* SIAM J. Appl. Dyn. Syst., 3 (2004), pp. 1–68.

[46] J. A. Sherratt, M. J. Smith, and J. D. M. Rademacher, *Patterns of sources and sinks in the complex Ginzburg–Landau equation with zero linear dispersion,* SIAM J. Appl. Dyn. Syst., 9 (2010), pp. 883–918.

[47] L. Brevdo, *A study of absolute and convective instabilities with an application to the Eady model,* Geophys. Astrophys. Fluid Dyn., 40 (1988), pp. 1–92.

[48] L. Brevdo and T. J. Bridges, *Absolute and convective instabilities of spatially periodic flows,* Phil. Trans. R. Soc. Lond. A, 354 (1996), pp. 1027–1064.

[49] B. Sandstede and A. Scheel, *Absolute and convective instabilities of waves on unbounded and large bounded domains,* Phys. D, 145 (2000), pp. 233–277.

[50] R. J. Briggs, *Electron-Stream Interaction with Plasmas,* MIT Press, Cambridge, MA, 1964.

[51] M. L. Rosenzweig and R. H. MacArthur, *Graphical representation and stability conditions of predator-prey interactions,* Am. Nat., 97 (1963), pp. 209–223.